Regular Article

Mechanism of angular momentum transfer from microwaves to a copper ring

Olivier Emile[1,a], Ronan Niemiec[1,2], Christian Brousseau[2], Janine Emile[3], Kouroch Mahdjoubi[2], Wenlong Wei[2], and Bo Thide[4]

[1] Université Rennes 1, 35042 Rennes Cedex, France
[2] UMR CNRS 6164 IETR, Université Rennes 1, 35042 Rennes Cedex, France
[3] UMR CNRS 6251 IPR, Université Rennes 1, 35042 Rennes Cedex, France
[4] Swedish Institute of Space Physics, Ångström Laboratory, P.O. Box 537, 751 21 Uppsala, Sweden

Abstract. In the exchange of orbital angular momentum between an electromagnetic wave and a copper ring we examine the origin of the Angular Momentum. We then investigate the transfer mechanism between the microwave and the object, and compare it with other mechanisms. We evidence a transfer mechanism based on the reflection of the electromagnetic field on the copper ring. In particular, at a microscopic scale, we show that the electromagnetic field induces alternative electric currents in the ring, with a small drift. Although little, the resistivity of copper leads to a force that rotates the ring. The estimation of the torque, which is of the order of 10^{-8} Nm, is in good agreement with the experimental measurements. We also show that the transfer of electromagnetic orbital angular momentum to objects could be a way to measure the orbital angular momentum carried by electromagnetic fields, and we discuss possible applications.

1 Introduction

Since Beth pioneering experiments [1,2] on the transfer of angular momentum (AM) between electromagnetic waves and macroscopic objects, there have been several studies reporting mechanical torques on various objects. Whereas some works manipulate the radiation pressure on specifically designed complex objects [3–5], most of the experiments use the AM of light. It can either be the spin angular momentum (SAM) in the microwave domain [6,7] and in the optical domain with macroscopic [8] and microscopic objects [9–11], or the orbital angular momentum (OAM). The latter has only been evidenced in the optical domain, with micro particles [12–14] and Bose-Einstein condensates [15]. The objects to be rotated could be birefringent particles or absorbing particles in the case of SAM exchange, and mostly absorbing particles in the case of OAM. Indeed, purely transparent particles do not change the helical phase front and hence do not interact with OAM, except when they induce astigmatism or when light is scattered [16]. The origin of the transfer mechanism, in terms of torque, was difficult to interpret for birefringent particles for SAM [17], but it has now been elucidated [18–20]. It is also clear for absorption, for SAM and/or OAM. Recently, we have reported the transfer of AM to a copper ring in the centimeter range [21] at 870 MHz. Since the copper ring only little absorbs radiations at this wavelength, one may then wonder what the transfer mechanism is. The aim of this article is thus to investigate the electro-magnetic field (EM) and the current in the copper ring, to try to elucidate the AM transfer to the object and then to estimate the torque exerted on the ring. After describing the experimental set-up (see Sect. 2), and recalling few theoretical results (see Sect. 3), we present the experimental results in Section 4. We then discuss them and focus on the transfer mechanism. We finally compare it with other transfer mechanisms (see Sect. 5) before reaching the conclusion.

2 Experimental set-up

The experimental set-up, which has already been described in [21], is sketched in Figure 1. This is an adaptation of the proposal made several years ago by Vulf'son [22]. The EM field carrying OAM is generated by a so-called turnstile antenna [23] made of two 17-cm-long, 2-mm-diameter copper dipole antennas. According to the Voltage Standing Wave Ratio (VSWR), which describes the adaptation of the antenna impedances to the transmission lines they are connected to, we decided to perform the experiment at a frequency $\nu = 870$ MHz (see insert of Fig. 1).

A -3 dB coupler splits the signal generated from a sinusoidal frequency synthesizer in two, and induces a

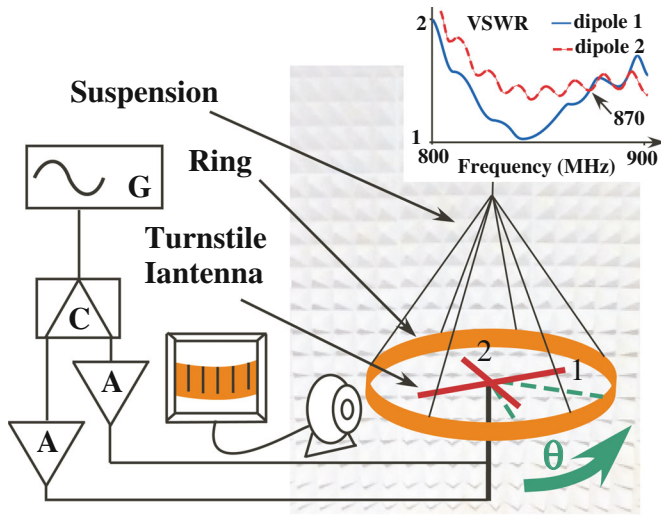[a] e-mail: olivier.emile@univ-rennes1.fr

Fig. 1. Experimental set-up. G: radio frequency generator, C: -3 dB coupler, A: 40 dB amplifier. The experiment is performed in an anechoic chamber. Inset VSWR versus frequency for the two dipole antennas. The arrow at a frequency of 870 MHz corresponds to the crossing of the two VSWR signals.

$\phi_1 - \phi_2 = \pi/2$ phase between the outputs. The two signals are amplified by two 40 dB gain amplifiers and then sent to the antennas. The maximum total output for each dipole is 25 W. This turnstile antenna is usually used to radiate a circularly polarized field in the axis of the antenna. However, it also radiates an electric field carrying OAM in the plane of the antenna. We are here interested in this last case.

The rotating object is a copper ring (radius $R = 150$ mm, height $H = 50$ mm, thickness $T = 0.165$ mm). Its polar moment of inertia is $J = 8.4 \times 10^{-4}$ kg m^2. The suspension is a 2-m-long, 0.5-mm-diameter cotton thread, fixed to the ceiling. Its torsion constant is measured from the 12-min-period of the free oscillations of the pendulum. It equals $C = 5.6 \times 10^{-8}$ N.m/°. To avoid any spurious EM effect, the experiment is confined in an anechoic chamber dedicated to this frequency range. Special care is taken to isolate the set-up from any mechanical vibration. An angular graduation is glued on the copper ring, and the rotation is recorded on a computer via a webcam.

3 Theoretical considerations

3.1 Expression of the EM field

We have calculated the electric field radiated in the plane of the antenna using CST simulation software [24], taking into account the near and the far field components of the field. The results of these simulations are shown in Figure 2. Figure 2a presents the amplitude of the electric field and Figure 2b corresponds to its phase. Whereas the amplitude decreases according to a $1/r$ law in the far field, as for the usual field radiated by a dipole [25], the phase
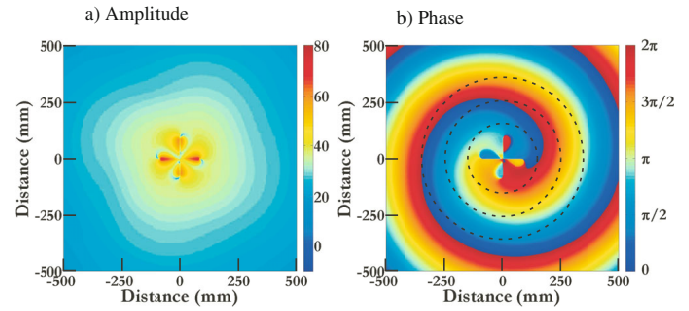

Fig. 2. Plot of the amplitude (a) in logarithmic scale (dB (V/m) units), and phase (b) of the electric field radiated by the turnstile antenna in the plane of the antenna, without the copper ring. The dotted concentric circles of figure b are guides for the eye to exemplify the 2π phase rotation.

variation is very differently from a single dipole antenna. On concentric circles aligned on the center of the antenna (dotted lines in Fig. 2b), the phase has a 2π variation in one turn. It thus seems that the EM field indeed carries OAM and that the topological charge ℓ is equal to 1.

On the other hand, the electric field could be analytically calculated. This has already been done in [21], and can be also found in the literature, see for example [26] and references therein. We have recalled the main results of the calculations in order to express the AM and we have fixed a few inaccuracies. However, in the following, the formula expressing the infinitesimal orbital (Eq. (5)), spin (Eq. (7)) and total AM for the ring (Eq. (8)) were not derived previously, neither the torque in the following paragraph (Eq. (9)). We use the cylindrical coordinates (ρ, θ, z), the origin O being at the center of the turnstile antenna, $\mathbf{e_z}$ being perpendicular to it. The complex vector potential, in the plane of the turnstile antenna, writes at a point M

$$\mathbf{A}(M,t) = -\frac{\mu_0}{4\pi}\frac{j\omega}{r}p_0 e^{j(kr-\omega t)}e^{j\theta}(\mathbf{e}_\rho + j\mathbf{e}_\theta), \quad (1)$$

where $r = OM$, ω is the pulsation of the current, p_0 is the dipole moment, μ_0 is the magnetic permeability and k is the wave vector modulus. The complex magnetic field then writes

$$\mathbf{B}(M,t) = -\frac{\mu_0}{4\pi}\frac{j\omega}{r^2}p_0(1-jkr)e^{j(kr-\omega t)}e^{j(\theta-\pi/2)}\mathbf{e_z}. \quad (2)$$

The complex electric field writes

$$\mathbf{E}(M,t) = \frac{e^{j\theta}}{4\pi\epsilon_0}\frac{p_0}{r^3}e^{j(kr-\omega t)}\left[\begin{array}{l}2(1-jkr)\mathbf{e}_\rho - \\ j(1-jkr-k^2r^2)\mathbf{e}_\theta\end{array}\right], \quad (3)$$

ϵ_0 being the electric permittivity. These analytical expressions also correspond to the simulations of Figure 2 that have been performed with CST. One can note in equation (3) that, for a given distance r from the turnstile antenna, the modulus of the electric field is constant, its direction rotates around z, and its phase varies as a function of θ, from 0 to 2π in one turn. This is in agreement with simulations and experiments that have been performed on radial slot antennas [27], in a different configuration.

3.2 Expression of the angular momenta

Let us calculate the AM density and the associated torque. This last point has not been completely elucidated previously in [21]. From equations (2) and (3), one evaluates the total AM density $\mathbf{w_T}$ taking the real part of the EM fields, $\mathbf{w_T} = \epsilon_0 \mathbf{r} \times (\mathbf{E} \times \mathbf{B})$, [25,26,28], in the plane of the antenna at a point M. This is nothing but the vectorial product of the Poynting vector by $\mathbf{r}$. Since $\mathbf{B}$ is along $\mathbf{e_z}$ and $\mathbf{r}$ is along $\mathbf{e}_\rho$, one has only to consider the component of the electric field along $\mathbf{e}_\rho$, which indeed corresponds to a near field component. One gets

$$\mathbf{w_T}(M,t) = \frac{2\mu_0\omega}{(4\pi)^2}\frac{p_0^2}{r^4}\begin{bmatrix} \cos^2(kr-wt+\theta)+ \\ k^2r^2\sin^2(kr-wt+\theta)+ \\ 2kr\cos(kr-wt+\theta)\times \\ \sin(kr-wt+\theta) \end{bmatrix}\mathbf{e_z}.$$

(4)

In order to calculate the torque exerted on the ring, one has to evaluate the infinitesimal AM $d\mathbf{J_r}$ passing through the ring during dt. Then one has to integrate equation (4) over the whole ring and estimate the AM crossing the ring during dt. This corresponds to a multiplication by cdt. As one integrates over θ, $rd\theta$ being the elementary length, the $\cos^2$ term averages to π, as well as the $\sin^2$, whereas the $\sin \times \cos$ averages to zero. Assuming that the EM field keeps the same expression on the whole height H of the ring as the one in the plane of the antenna (we have indeed checked numerically, that the variations in amplitude and in phase are less than 5%), this leads to a total AM on the ring that equals to

$$d\mathbf{J_r} = \frac{2\mu_0\omega}{(4\pi)^2}\frac{p_0^2}{r^3}\pi Hcdt\left[1+k^2r^2\right]\mathbf{e_z}.$$

(5)

Similarly, one can calculate the SAM. To avoid any gauge choice dilemma [25,28], one has to evaluate the SAM density $\mathbf{w_S} = \epsilon_0\mathbf{r}\times(\mathbf{E}\times\mathbf{A})$ considering the transverse component of the vector potential only. Then, from equations (1) and (3), one gets

$$\mathbf{w_S}(M,t) = \frac{\mu_0\omega}{(4\pi)^2}\frac{p_0^2}{r^4}\begin{bmatrix} 2\cos^2(kr-wt+\theta)+ \\ kr\cos(kr-wt+\theta)\times \\ \sin(kr-wt+\theta) \end{bmatrix}\mathbf{e_z}.$$

(6)

One also estimates the infinitesimal SAM $d\mathbf{S_r}$ exerted on the ring following the same procedure as above. This leads to

$$d\mathbf{S_r} = \frac{2\mu_0\omega}{(4\pi)^2}\frac{p_0^2}{r^3}\pi Hcdt\mathbf{e_z}.$$

(7)

From equations (5) and (7), one deduces the infinitesimal OAM exerted on the ring. It is simply

$$d\mathbf{L_r} = d\mathbf{J_r} - d\mathbf{S_r} = \frac{2\mu_0\omega}{(4\pi)^2}\frac{p_0^2}{r}k^2\pi Hcdt\mathbf{e_z}.$$

(8)

It has to be noted that the OAM has the same expression in the near field and in the far field, assuming that the height of the ring increases linearly with r as one moves further up.

3.3 Estimation of the topological charge

Although equation (4) clearly shows that the phase of the electric field has a 2π variation in one turn, one may wonder whether the value $\ell = 1$ of the topological charge could be confirmed using equation (8).

Let us imagine that OAM would have kept the same expression as the one found in the plane of the turnstile antenna. We now evaluate the torque over an infinite cylinder. Let us call ϕ the angle between the plane of the antenna and the radial vector (H is replaced by $r\sin\phi d\phi$ in the OAM density). Since one considers the projection of the AM over the z axis, one should add a $\cos\phi$. Finally, for a given ϕ, the OAM passing through the cylinder corresponds to thickness $c\cos\phi dt$. Then one would have to integrate $\cos^2\phi\sin\phi d\phi$ between 0 and $\pi/2$ corresponding to a half infinite cylinder and to multiply by a factor of 2 to get the whole cylinder. This would lead to a factor 2/3. Then, the available torque would be

$$\frac{d\mathbf{L_r}}{dt} = \frac{4}{3}\frac{\mu_0\omega}{(4\pi)^2}p_0^2ck^2\pi\mathbf{e_z}.$$

(9)

From a general point of view, an EM field with a power P and a topological charge ℓ exerts a torque that is

$$\Gamma_{th} = \ell P/\omega.$$

(10)

Such power is related to the dipole moment [23] by the relation

$$P = \frac{1}{12\pi\epsilon_0 c^3}p_0^2\omega^4,$$

(11)

then comparing this expression with equation (9), this would lead to

$$\|\frac{d\mathbf{L_r}}{dt}\| = P/\omega,$$

(12)

which indeed corresponds to a topological charge equal to $\ell = 1$. This confirms that the OAM associated to the EM field in the plane of the antenna has a topological charge equal to $\ell = 1$. It has been here estimated by the available torque in a manner similar to what has been done in acoustics [29]. This torque is a multiple integer of the radiated power. Then, the measurement of the OAM carried per photon leads to an integer number times $\hbar$, $\hbar$ being the reduced Plank constant.

3.4 Paradox

However, the expression of the electric field could be viewed as a kind of a paradox. Indeed, if one considers the far field only in equation (3), or if one moves in the far field region, the electric field writes

$$\mathbf{E}(M,t) = \frac{1}{4\pi\epsilon_0}\frac{p_0}{r}e^{j(kr-\omega t)}e^{j\theta}jk^2\mathbf{e}_\theta.$$

(13)

The electric field is tangential. From equation (2) the magnetic field is vertical. The Poynting vector is thus radial. This erroneous back-of-an-envelope calculation would lead
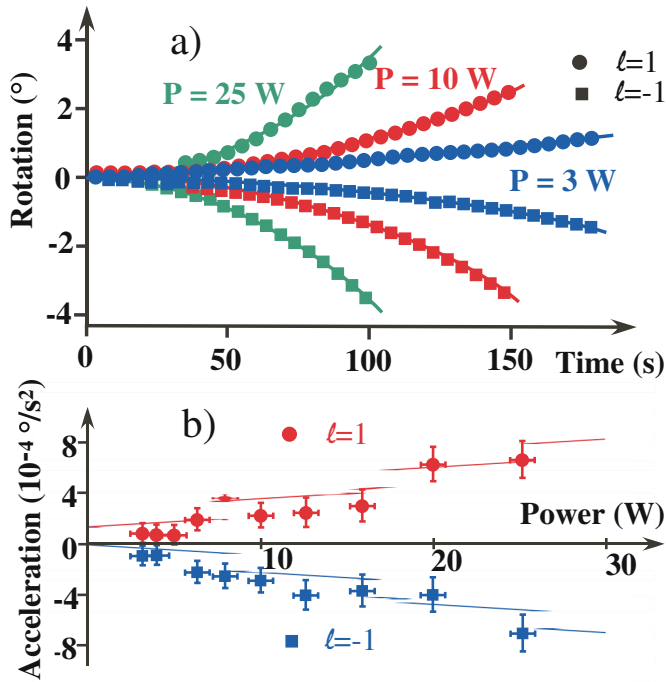
Fig. 3. (a) Rotation versus time for a $\pi/2$ (circle) and $-\pi/2$ (square) phase between the two dipole antennas for different transmitted powers. (b) Acceleration versus power for a $\pi/2$ (circle) and $-\pi/2$ (square) phase between the two dipole antennas.

to an OAM equal to zero, since the OAM is the vectorial product of the radial vector and the Poynting vector. Indeed, the radial component of the electric field (which is usually said to be the near field component) only contributes to the OAM, even in the far field.

The same kind of paradox also holds for Beth experiment [2] for SAM. In that case, a plane wave crosses a half wave plate. Rapidly estimating the SAM, one would say that the Poynting vector is along the propagation direction. This cannot induce any torque on the plate which is perpendicular to the propagation direction. This paradox has been solved in [18]. The light beam could be Gaussian thus having components not parallel to the propagation direction, or the plate could have finite dimensions thus creating diffraction and components non parallel to the propagation direction. As a result, the components of the Poynting vector which are not parallel to the propagation direction, only contribute to the torque.

4 Experimental results

The experimental results have already been presented in [21]. We have evidenced a uniformly accelerated rotation of the pendulum, as can be seen from Figure 3. In Figure 3a we have plotted the rotation versus time for three different powers. The rotation depends on the power, as expected. As the phase between the two dipole antennas is reversed from $+\pi/2$ to $-\pi/2$, the sign of the OAM

switches from $\ell = 1$ to $\ell = -1$. The sign of the torque then also changes. We find experimentally a change of the rotation direction of the pendulum. Besides, the two plots of the rotation are nearly perfectly symmetric. When the two dipole antennas are in phase, no rotation is observed.

Figure 3b shows the angular acceleration induced by the EM field versus the transmitted power to each dipole. The experimental results evidence a linear dependence versus the power, as expected, that holds over one order of magnitude. Note also that the linear coefficient is exactly reverse for the other rotation direction. From Figure 3b, for a 25 W power, we find an acceleration of 7.8×10^{-4} °/s² which corresponds to an OAM torque of $\Gamma_{ex} = 1.1 \times 10^{-8}$ Nm.

5 Discussion

5.1 Comparison between experiment and theory

According to the theoretical section (Eq. (10)), assuming that the total radiated power P_t is twice the power emitted by each dipole (which is of course an over estimation), the maximum torque available would be

$$\Gamma_{th} = \hbar N = \hbar(P_t/h\nu) = P_t/\omega = 9.2 \times 10^{-9} \text{ Nm}, \quad (14)$$

where N is the number of photons emitted per second, assuming that all photon are used and that they have the same AM. At first glance, there is a very good agreement between this theoretical value Γ_{th} and the experimental one Γ_{ex}. However, the height of the ring is only 50 mm, at a distance of 150 mm, which leads to a solid angle that equals $\pi/3$, whereas Γ_{th} is estimated for an isotropic radiation with a solid angle that equals 4π. Then, the theoretical value seems to be more than one order of magnitude under estimated.

5.1.1 Fabry-Perot effect

First, the ring is made of copper which is a nearly perfectly reflecting material at this frequency. It is usually assumed that for a perfectly electrical conductor, no AM transfer by reflection could be performed [30–32]. Indeed, following the arguments given in these references, to ensure continuity of the fields, the tangential component of the electric changes sign upon reflection, thus excluding any inversion of the AM. Because of AM conservation, no transfer can then be performed. Nevertheless, in our case, the OAM is due to the longitudinal component of the electric field which does not change its sign upon reflection, enabling for OAM change and AM transfer. This is the same argument as the one used in [32] for SAM transfer at oblique incidence. This leads to a transfer of $2\hbar$. This can be evidenced in Figure 4, where we have plotted the equi-phase of the electric field for different times.

Second, the ring is at a distance $R = 150$ mm from the source, that is of the order of $\lambda/2$, i.e. still in the near field. The copper ring thus interacts with the totality
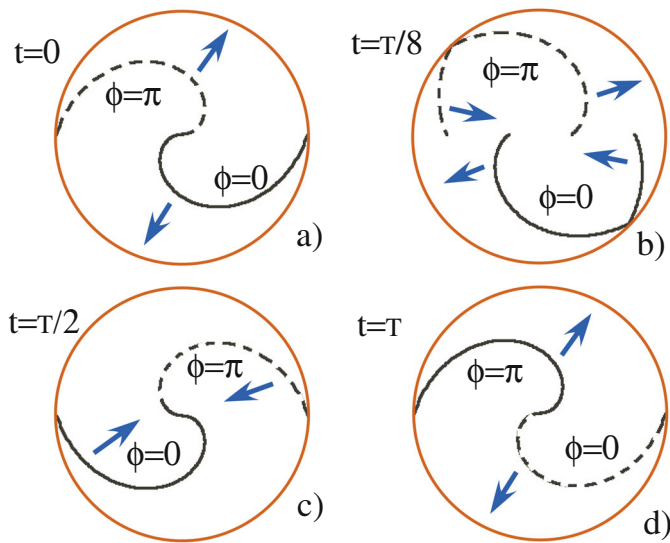
Fig. 4. Interference effect. Evolution of phase fronts of the electric field in the plane of the antenna, for a phase front $\phi = 0$ (solid line) and $\phi = \pi$ (dotted line) for (a) $t = 0$, (b) $t = T/8$, T being the period, (c) $t = T/2$ and (d) $t = T$. Upon reflection ($t = T/2$), the sense of rotation of the electric field has changed. After a period, the field corresponds to the field at $t = 0$. Thus the field interferes constructively. Bold blue arrows show the direction of the propagation of the wave.

Fig. 5. Amplitude of the electric field in the plane of the antenna, in presence of the ring, in logarithmic scale (dB (V/m) units). The radius of the ring corresponds to the experimental value $R = 150$ mm.

of the field. One has to consider the antenna and the field as a whole. In order to check this hypothesis, we have carried out calculations still using CST software taking into account the antenna and the ring. The results can be seen in Figure 5. Actually, one can notice that in the plane of the antenna, there is hardly any field radiated outside the strip location. All the field is concentrated inside the strip.

Third, since the diameter of the ring equals λ, the copper ring behaves as a Fabry-Perot. As already discussed, the topological charge of the AOM is reversed upon reflection. It is again reversed when crossing the center of the turnstile antenna which is at the focus of the reflecting ring. Indeed, when crossing this focus, the longitudinal component of the electric field remains unchanged. Due to the so-called Gouy phase [33], the magnetic field experiences a $\pi/2$ phase shift for a $\ell = 0$ Gaussian beam. This is exactly the same experimental situation as the one encountered with acoustical waves [34] where they evidenced also a $\pi/2$ phase shift for a spherical wave in two dimensions. For a $\ell = 1$ topological charged beam, there is an extra $\pi/2$ phase shift [35]. Thus the magnetic field changes its sign crossing the focus, leading to a change of the topological charge, in a manner similar to what can be found in optics for cylindrical lenses [36]. This can be evidenced also in Figure 4. After the focus, the topological charge is the same as for the incoming beam. Since the tangential component of the electric field also changes it sign due to the Gouy phase, the reflected field interferes constructively with the incoming beam, leading to a Fabry-Perot effect.
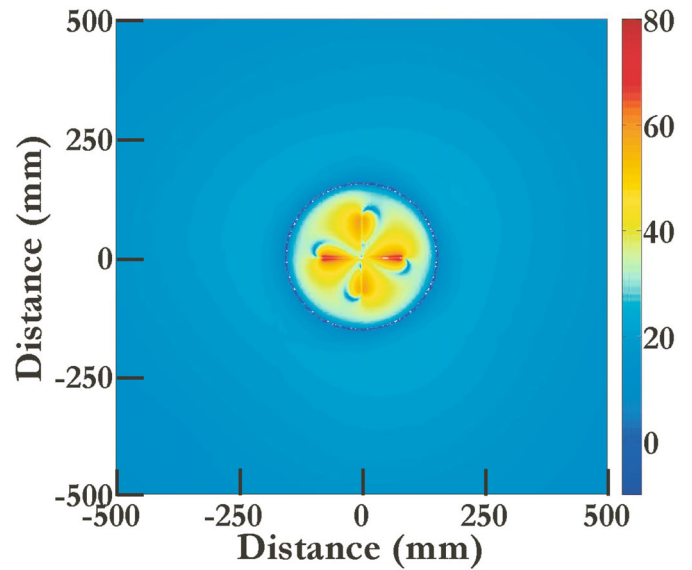
Yet, because the same EM wave serves several times to rotate the ring, one may wonder whether energy conservation might be violated. Indeed, the reflected wave, due to the rotational Doppler effect [37], has a slightly lower frequency. The increase of the energy of the ring due to rotation is compensated by a lowering of the photon energy that enables energy conservation. Could this variation be detected? For a 1 Hz rotation frequency of the ring, which is far above the rotation frequency our pendulum could experience, the rotational Doppler shift would be of 1 Hz. Compared with the 1 GHz microwave frequency we used in our experiment, it is a 10^{-9} relative variation. This is much lower than the natural width of our frequency synthesizer which is of the order of 100 Hz. The frequency change is hardly noticeable in our case and must be difficult to unambiguously isolate and to determine.

Since the strip lies in the near field, it is quite difficult to estimate the finesse of this radio frequency Fabry-Perot. We have tried to determine it experimentally. Due to high losses, the photons are only bouncing a few times. The finesse should be lower than ten, that is a very low finesse. Then the width of the transmission resonance frequency must be very broad, of the order of few tens of megahertz. Performing experiments, the only resonance we evidenced when we changed the excitation frequency was the width of the frequency response of the antennas which is of the order of 10 MHz (see insert of Fig. 1).

As for a usual Fabry-Perot in optics, and according to Figure 5, the ring position corresponds to a node of the interfering waves. The electrons within the metal react so as to ensure EM field continuity. Since the field is equal to zero at the strip location the transfer mechanism could not be via absorption as supposed in [22]. It must be by reflection. However, the argument given above doesn't explain the transfer mechanism at a microscopic scale, neither the
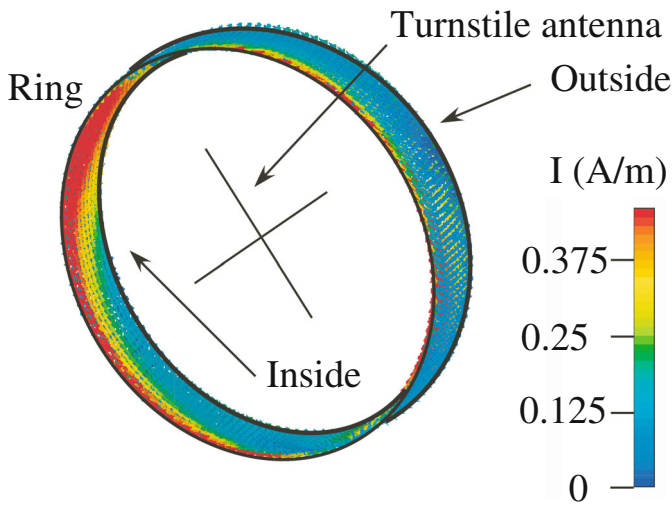
Fig. 6. Simulated distribution of the electric current on the copper ring at a given time for our experimental set-up, for a radiated power of 25 W. Note that the current is running inside the ring. There is hardly any current running outside.

Fig. 7. Integration of the differential equation (Eq. (15)) for a radiated power of 25 W. The electrons are submitted to an oscillatory force at the frequency of the EM field and a drift that is due to the OAM.

discrepancy between the expected torque values and the experimental observations. The EM waves must anyhow interact with the copper ring. Since EM waves cannot penetrate below the surface of the ring, the Lorentz force of the light can only act on the charges and the currents at the surface of the ring [32]. The next paragraph is dedicated to discuss the transfer mechanism in terms of currents, taking all these effects into account.

5.1.2 Transfer mechanism

At the strip location, the tangential component of the EM field induces an alternative current I running at the surface of the strip with a $\cos(\theta - \omega t)$ variation (see Eq. (3)). This current experiences a resistance thus generating an electric field that drives the copper atoms. These atoms then radiate an EM field to compensate for the incoming field. Following Newton's second law of mechanics, considering a small portion of the ring, one finds that

$$\frac{d^2\theta}{dt^2} = \frac{\rho_q \rho I}{\rho_m R H T} \cos(\theta - \omega t) = a \cos(\theta - \omega t), \qquad (15)$$

where ρ_q is the charge density, ρ_m is the mass density, ρ is the copper resistivity. We have plotted the intensity of the current at a given time on the ring still using CST software, taking into account the influence of the ring. The result is displayed in Figure 6. One can clearly see that there is an oscillating current running on the inner side of the copper ring only. With these simulations we are able to estimate the amplitude of the current.

This current is found to be $I = 0.25$ A, leading to $a = 5.5 \times 10^3$ °/s². This value is the amplitude of the oscillating term in equation (15). It is not directly linked to the average acceleration experienced by the ring. One has then to solve the differential equation. Indeed, a temporal
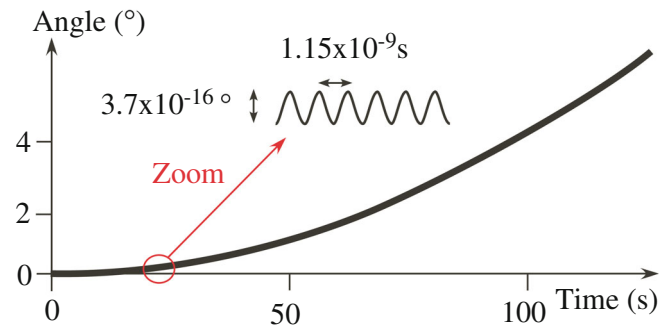
variation of the form $\cos(\omega t)$ would have lead to the collective oscillations of the atoms of the copper ring at the EM field frequency. However, the presence of θ in equation (15) also leads to a position drift. We have plotted in Figure 7 the numerical solution of equation (15) with the experimental values. One can clearly identify two regimes. The first one corresponds to an oscillation of the mobile with the frequency of the radiated field. This oscillation would have been present even with a plane wave. However, at longer time scales, there is a drift of this oscillation. Actually the electrons are drifted due to the existence of the phase variation of the electric field. The angle variation resembles a parabola.

From equation (15), there seems to be a self contradiction between Section 5.1.1 and the current Section 5.1.2. In Section 5.1.1, we claim that the transfer mechanism is via reflection whereas in this paragraph we introduce a dissipation mechanism via the copper resistivity in a way that resembles to absorption.

Here, the transfer mechanism is clearly via reflection. It can't be via absorption for the two following reasons. First, in a perfectly conducting material, the running currents at the ring surface would tend towards infinity. The currents are proportional to the inverse of the resistivity. There must be a dissipation mechanism within the copper that accounts for the interaction of the "free" electrons of the metal and the periodic structure. This enables AM conservation. However this absorption is far too weak to be the main transfer mechanism. Indeed, since the reflection coefficient in intensity of copper is of the order of $99,99\%$ [23], the absorption is in the 0.01% range or lower. Then if we considered this absorption from the total available power, which is of course an over estimation, this would lead to a torque of the order of $\Gamma_{abs} = 10^{-4} \times \hbar N = 9.2 \times 10^{-13}$ Nm. This is negligible. Second, as explained in the beginning of Section 5.1, there is not enough power available even if all the power is absorbed and transformed to AM to explain our observations.

5.1.3 Torque estimation

From the numerical integration of equation (15), that appears in Figure 7, we estimate the angular acceleration

of the ring to $a_m = 8.2 \times 10^{-4}$ °/s². The corresponding torque is of the order of $\Gamma_{cal} = 1.2 \times 10^{-8}$ Nm. This value is in very good agreement with the experimental value $\Gamma_{ex} = 1.1 \times 10^{-8}$ Nm. This thus validates the fact that the turnstile antenna and the copper ring should be considered as a whole system as calculated in Figure 5. It also validates that the ring behaves like a Fabry-Perot interferometer. This Fabry-Perot effect could not have been taken into account in the calculation carried out in Section 3.3.

From equation (15), since I varies linearly with the frequency, one may think that the torque varies accordingly contrarily to equation (14). However, the numerical integration of equation (15) gives a factor proportional to the inverse of the square of the pulsation, leading to a linear dependence of the torque with the wavelength.

5.2 Discussion of the transfer mechanism

5.2.1 Comparison with other transfer mechanisms

The rotation of small objects by light sources can be induced either by the linear momentum or by the AM. The first scheme takes advantages of specially shaped three-dimensional objects and the scattering of ordinary light [4,38,39]. The radiation pressure or/and the scattered light exert a force that leads to a torque on such objects. In addition to this mechanism, one can refer to thermocapillary propulsion observed for asymmetric microgears [40] where the heat transfer due to the light absorption leads to a torque effect. One can also mention the diffraction of a plane wave on an asymmetric object, [41,42], where the diffracted light carries OAM. Nevertheless, we are interested here in the transfer of momentum from light carrying AM to objects. As for the second scheme, the mechanisms of OAM transfer between light carrying AM and objects can be considered under two different aspects. The first one relies on the determination of the origin of the torque, whereas the second one considers the AM conservation that must be always fulfilled [43]. We are interested here in both aspects.

For SAM, the rotating objects could be birefringent or absorbing objects. In the case of absorbing objects, the torque is applied by the absorbed light and the AM conservation implies that each absorbed photon transfers $\hbar$. In the case of birefringent objects, as discussed in Section 3.4, diffraction is responsible for the torque. In the ideal case of $\lambda/2$ birefringent objects, each circularly polarized photon flips its polarization leading to a $2\hbar$ per photon transfer. It could even be increased by a factor of 2 by adding a $\lambda/4$ plate and a mirror [1,8]. Birefringent particles could also follow adiabatically (in a quantum mechanical sense, see for example [44]) a rotating polarization [9,45].

For OAM, the transfer mechanism for absorbing or reflecting particles relies in the twisting photons around their propagation direction. Then each photon transfers $\hbar$ for absorption and $2\hbar$ for reflection as in our case. For transparent objects the problem is of a different nature. As already stated in the introduction, for purely transparent particles, the helical phase of the incident beam is not changed while crossing the objects. Hence the objects cannot interact with OAM [16]. However, when these objects introduce astigmatism, the phase front is modified and OAM could be transferred [46]. Besides, in those latter cases, scattering or diffraction of OAM by these objects, could be the transfer mechanism. Nevertheless, scattering and diffraction also modify the helical wavefront and the objects couldn't be considered as purely transparent any more. For example, a "free" cylindrical lens could rotate under the influence of an OAM field [36]. As for birefringent objects, micro-particles can also be trapped in patterns that are rotating. These particles would then follow adiabatically the pattern rotation at a low frequency of the order of few Hertz [47,48]. However such mechanical rotation is not directly linked to the OAM of light.

There is another OAM transfer mechanism based on coherent processes that has been applied to atoms. In particular, the OAM carried by a pump beam could be absorbed by an atom and then probed in a four wave mixing experiment [49]. In the case of Bose Einstein condensates, the absorption of a photon in an incident OAM carrying beam could transfer OAM to the condensate by a resonant two photon process [15]. In such processes, the transfer mechanism relies also on absorption. Nevertheless, in a two photon process, both beam could carry OAM [50]. Then the transfer mechanism is induced both by absorption and stimulated emission. It could also be the same mechanism for ions [51].

In our case, the transfer mechanism is clearly via reflection via a $2\hbar$ transfer by reflected photon. The reflected beam induces a current inside the rotating strip that causes the mobile to rotate. It is very different from other mechanisms of AM transfer. This transfer mechanism resembles the transfer of AM in the case of the induction motor for magnetic field [52]. Since the detection of a tiny current can be easily carried out, this kind of detection scheme can be an alternative to the determination of an OAM EM field.

5.2.2 Torque estimation as a measure of the topological charge of a twisted beam

In optics, the precise determination of the OAM is still a challenging issue [53,54], for example in highly focused geometry or for large values of ℓ [55]. There are mainly three different existing ways to measure the OAM carried by an EM field. The method we have described here could be considered as a fourth method.

The most commonly used method is via interferences either with a plane wave [56–58] or with self interferences [59–64], or even considering the light speckle [65]. An alternative to measure OAM is by optical transformation, operating for example the mode creation optics in reverse [56,66–69]. These two techniques could be called classical optical methods. The third method uses the rotational Doppler shift of the beam [70]. It is linked to the EM field-matter interaction. The fourth method also relies on EM field-matter interaction. It measures both the torque and the applied power to deduce the topological

charge. Such measurement leads to an integer value of the OAM quantity. It has been described in this article in microwaves, although it is coupled here with a Fabry-Perot effect. Besides, in order to measure the topological charge, we can here either measure the torque or the electrical current.

6 Conclusion

We have investigated the OAM transfer from the EM field radiated by a turnstile antenna in the plane of the antenna to a suspended copper ring. We have shown that the AM transfer mechanism is by reflection of the EM field on the conducting ring. Actually, the EM field induces a small oscillating current with a drift, in the ring. Due to this drift, the ring starts to rotate. The estimated torque is in reasonable agreement with numerical estimations and with the maximum torque available from the antenna. However, each photon must have been used several times like in a Fabry-Perot interferometer. As the sign of the topological charge is reverse, the sign of the torque is also reversed.

Such an experiment could be a new way to detect OAM. Actually, the topological charge can be either detected by the torque exerted on the pendulum like we did here, but it could also be done via the current generated on the detector. Since, in principle, very tiny current could be detected, this could lead to applications in the OAM detection especially in the radio domain where for a given power, the OAM varies linearly with the wavelength, and where the techniques used in optics do not always apply [71,72]. It could even be used to detect OAM in astronomy [73,74]. Conversely, it may also be applied in optics since light beams can generate static electric fields and current via nonlinear effects such as optical rectification [75,76].

Author contribution statement

OE, CB and BT conceived the experiment, CB, OE and RN did the experiments, OE and JE carried out the calculations, RN, KM and WL performed the simulations, OE, CB, JE, KM and BT discussed the results, and OE, JE and CB wrote the paper.

References

1. R.A. Beth, Phys. Rev. **48**, 471 (1935)
2. R.A. Beth, Phys. Rev. **50**, 115 (1936)
3. E. Higurashi, H. Ukita, H. Tanaka, O. Ohguchi, Appl. Phys. Lett. **64**, 2209 (1994)
4. P. Galajda, P. Ormos, Appl. Phys. Lett. **78**, 249 (2001)
5. M. Padgett, R. Bowman, Nat. Photon. **5**, 343 (2011)
6. N. Carrara, Nature **164**, 882 (1949)
7. P.J. Allen, Am. J. Phys. **34**, 1185 (1966)
8. G. Delannoy, O. Emile, A. Le Floch, Appl. Phys. Lett. **86**, 081109 (2005)
9. M.E.J. Friese, T.A. Nieminen, N.R. Heckenberg, H. Rubinsztein-Dunlop, Nature **86**, 348 (1998)
10. B.E. Kane, Phys. Rev. B **82**, 115441 (2010)
11. F. Pedaci, Z.X. Huang, M. van Oene, S. Barland, N.H. Dekker, Nat. Phys. **7**, 259 (2011)
12. H. He, M.E.J. Friese, N.R. Heckenberg, H. Rubinsztein-Dunlop, Phys. Rev. Lett. **75**, 826 (1995)
13. S. Franke-Arnold, L. Allen, M. Padgett, Laser Photon. Rev. **2**, 299 (2008)
14. D.B. Ruffner, D.G. Grier, Phys. Rev. Lett. **108**, 173602 (2012)
15. M.F. Andersen, C. Ryu, P. Cladé, V. Natarajan, A. Vaziri, K. Helmerson, W.D. Phillips, Phys. Rev. Lett. **97**, 170406 (2006)
16. A.M. Yao, M.J. Padgett, Adv. Opt. Photon. **32**, 161 (2011)
17. J.M. Jauch, F. Rohrlich, *the theory of photons and electrons* (Addison-Wesley, New York, 1955)
18. J.W. Simmons, M.J. Guttmann, *States, Waves and Photons* (Addison-Wesley, Reading, MA, 1970)
19. L. Allen, M. Padgett, Opt. Commun. **184**, 67 (2000)
20. A.M. Stewart, Eur. J. Phys. **26**, 635 (2005)
21. O. Emile, C. Brousseau, J. Emile, R. Niemiec, K. Madhjoubi, B. Thidé, Phys. Rev. Lett. **112**, 053902 (2014)
22. K.S. Vul'fson, Sov. Phys. Usp. **30**, 724 (1988)
23. J.D. Kraus, *Antennas*, 2nd edn. (McGraw-Hill, New York, 1988)
24. Computer Simulation Technology, CST, http://www.cst.com
25. B. Thidé, *Electromagnetic Field Theory*, 2nd edn. (Dover, NY, 2011), http://www.plasma.uu.se/CED/Book
26. B. Thidé, F. Tamburini, H. Then, C.G. Someda, R.A. Ravanelli, http://arxiv.org/abs/1410.4268 (2014)
27. K. Sudo, J. Hirokawa, M. Ando, Proc. 33rd Eur. Microwave Conf. **3**, 935 (2003)
28. S.J. van Enk, G. Nienhuis, J. Mod. Opt. **41**, 963 (1994)
29. C.E.M. Demore, Z.Y. Yang, A. Volovick, S. Cochran, M.P. MacDonald, G.C. Spalding, Phys. Rev. Lett. **108**, 194301 (2012)
30. C. Konzand, G. Benford, Opt. Commun. **226**, 249 (2003)
31. T.A. Nieminen, Opt. Commun. **235**, 227 (2004)
32. M. Mansuripur, A.R. Zakharian, E.W. Wright, Phys. Rev. A. **84**, 033813 (2011)
33. M. Born, E. Wolf, *Principles of optics* (Cambridge University Press, 1999)
34. A.A. Kolomenskii, S.N. Jerebtsov, H.A. Schuessler, Opt. Lett. **30**, 2019 (2005)
35. A.E. Siegman, *Lasers* (University Science Books, Mill Valley, CA, 1986)
36. G. Molina-Terriza, J. Recolons, J.P. Torres, L. Torner, Phys. Rev. Lett. **87**, 023902 (2001)
37. J. Courtial, D.A. Robertson, K. Dholakia, L. Allen, M.J. Padgett, Phys. Rev. Lett. **81**, 4828 (1998)
38. T.A. Nieminen, S.J.W Parkin, N.R. Heckenberg, H. Rubinsztein-Dunlop, Proc. SPIE **5514**, 254 (2004)
39. H. Rubinsztein-Dunlop, T. Asavei, A.B. Stilgoe, V.L.Y. Loke, R. Vogel, T.A. Nieminen, N.R. Heckenberg, in *Optical Nano and Micro Actuator Technology*, edited by G.K. Knopf, Y. Otani (CRC Press, 2012), pp. 277–306

40. C. Maggi, F. Saglimbeni, M. Dipalo, F. De Angelis, R. Di Leonard, Nat. Commun. **6**, 7855 (2015)
41. O. Emile, M. le Meur, J. Emile, Phys. Rev. A **89**, 013846 (2014)
42. O. Emile, J. Emile, Opt. Lett. **41**, 211 (2016)
43. F. Devaux, R. Passier, Eur. Phys. J. D **42**, 133 (2007)
44. M. Born, V. Fock, Z. Phys. **51**, 165 (1928)
45. S.L. Neale, M.P. MacDonald, K. Dholakia, T.F. Krauss, Nat. Mater. **4**, 530 (2005)
46. M.J. Padgett, L. Allen, J. Opt. Soc. Am. B **4**, S17 (2002)
47. L. Paterson, M.P. MacDonald, J. Arlt, W. Sibbett, P.E. Bryant, K. Dholakia, Science **292**, 912 (2001)
48. S. Franke-Arnold, J. Leach, M.J. Padgett, V.E. Lembessis, D. Ellinas, A.J. Wright, J.M. Girkin, P. Ohberg, A.S. Arnold, Opt. Express **15**, 8619 (2007)
49. J.W.R. Tabosa, D.V. Petrov, Phys. Rev. Lett. **83**, 4967 (1999)
50. J.F. Brachmann, W.S. Bakr, J. Gillen, A. Peng, M. Greiner, Opt. Express **19**, 12984 (2011)
51. C.T. Schmiegelow, F. Schmidt-Kaler, Eur. Phys. J. D **66**, 157 (2012)
52. P.W. Mattews, Am. J. Phys. **33**, 1082 (1965)
53. S. Franke-Arnold, J. Jeffers, Eur. Phys. J. D **66**, 196 (2012)
54. H. Qassim, F.M. Miatto, J.P. Torres, M.J. Padgett, E. Karimi, R.W. Boyd, J. Opt. Soc. Am. B **31**, A20 (2014)
55. R. Fickler, R. Lapkiewicz, W.N. Plick, M. Krenn, C. Schaeff, S. Ramelow, A. Zeilinger, Science **338**, 640 (2012)
56. V.Yu Bazhenov, M.S. Soskin, M.V. Vasnetsov, J. Mod. Opt. **39**, 985 (1992)
57. M. Harris, C.A. Hill, P.R. Tapster, J.M. Vaughan, Phys. Rev. A **49**, 3119 (1994)
58. M.P.J. Lavery, M.J. Padgett, in *Opical Angular Momentum*, edited by D.L. Andrews, M. Babiker (Cambridge University Press, London, 2012)
59. J. Leach, M.J. Padgett, S.M. Barnett, S. Franke-Arnold, J. Courtial, Phys. Rev. Lett. **88**, 257901 (2002)
60. J.M. Hickmann, E.J.S. Fonseca, W.C. Soares, S. Chávez-Cerda, Phys. Rev. Lett. **105**, 053904 (2010)
61. M.E. Anderson, H. Bigman, L.E.E. de Araujo, J.L. Chaloupka, J. Opt. Soc. Am. B **29**, 1968 (2012)
62. O. Emile, J. Emile, Appl. Phys. B **117**, 487 (2014)
63. O. Emile, J. Emile, C. Brousseau, J. Opt. **16**, 125703 (2014)
64. O. Emile, J. Emile, B. de Lesegno, L. Pruvost, C. Brousseau, Europhys. Lett. **111**, 34001 (2015)
65. M. Liu, Eur. Phys. J. D **67**, 244 (2013)
66. L. Allen, M.W. Beijersbergen, R.J.C Spreeuw, J.P. Woerdman, Phys. Rev. A **45**, 8185 (1992)
67. N.R. Heckenberg, R. McDuff, C.P. Smith, H. Rubinsztein-Dunlop, M.J. Wegener, Opt. Quantum Electron. **24**, S951 (1992)
68. M.W. Beijersbergen, L. Allen, H.E.L.O van der Veen, J.P. Woerdman, Opt. Commun **96**, 123 (1993)
69. G.C.G. Berkhout, M.P.J. Lavery, J. Courtial, M.W. Beijersbergen, M.J. Padgett, Phys. Rev. Lett. **105**, 153601 (2010)
70. J. Courtial, K. Dholakia, D.A. Robertson, L. Allen, M.J. Padgett, Phys. Rev. Lett. **80**, 3217 (1998)
71. B. Thidé, H. Then, J. Sjöholm, K. Palmer, J. Bergman, T.D. Carozzi, Y.N. Istomin, N.H. Ibragimov, R. Khanitova, Phys. Rev. Lett. **99**, 087701 (2007)
72. F. Tamburini, E. Mari, A. Sponselli, B. Thidé, A. Bianchini, F. Romanato, New J. Phys. **14**, 033001 (2012)
73. F. Tamburini, B. Thidé, G. Molina-Terriza, G. Anzolin, Nat. Phys. **7**, 195 (2011)
74. N.M. Elias, Astron. Astrophys. **541**, 101 (2012)
75. M. Bass, P.A. Franken, J.F. Ward, G. Weinreich, Phys. Rev. Lett. **9**, 446 (1962)
76. R.W. Boyd, *Nonlinear optics*, 3rd edn. (Academic Press, NY, 2008)